Electronic Supplementary Material (ESI) for Journal of Materials Chemistry A.

Supporting Information

A Metal-Organic Framework Film with Switchable Anodic and Cathodic Behavior in a Photo-Electrochemical Cell

Raya Ifraemov, Ran Shimoni, Wenhui He, Guiming Peng, Idan Hod*

Department of Chemistry and Ilse Katz Institute for nanoscale Science and Technology, Ben-Gurion University of the Negev, Beer-Sheva, 8410501, Israel.

E-mail: hodi@bgu.ac.il

Characterization Results

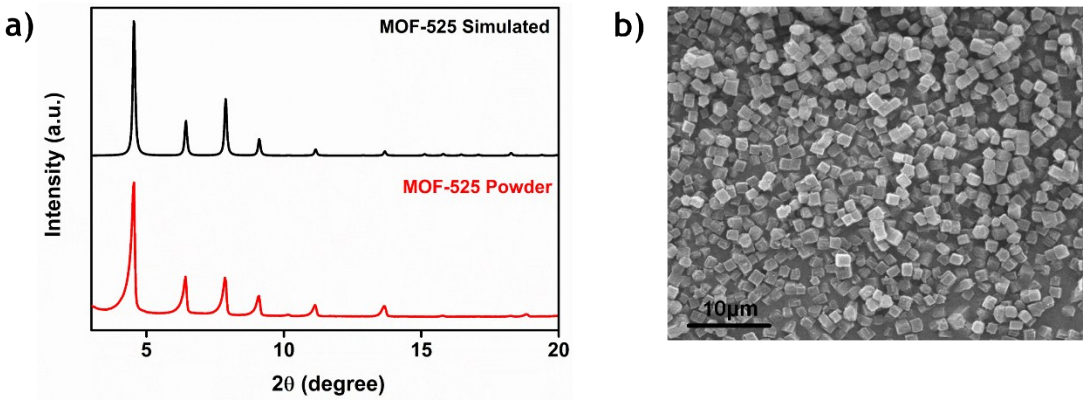

Figure S1. (a) XRD patterns of the simulated (black line) and as-synthesized (red line) MOF-525 powder (b) scanning electron microscopy images of the as-synthesized MOF-525 powder presenting its typical cubic morphology with the average size of 2 μm.

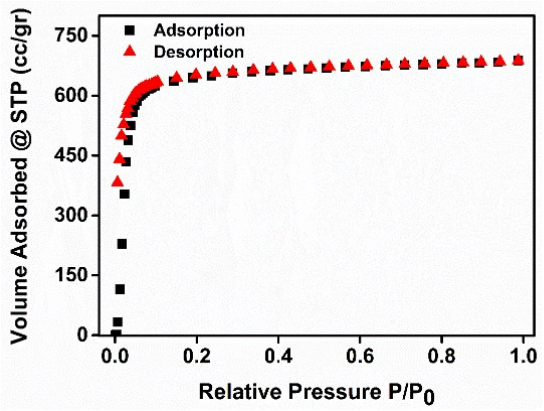

Figure S2. Nitrogen isotherm of MOF-525 powder at 77K after the sample was degassed at 120 °C in vacuum for 17 hours. The black curve represents the adsorption and the red the desorption measurement.

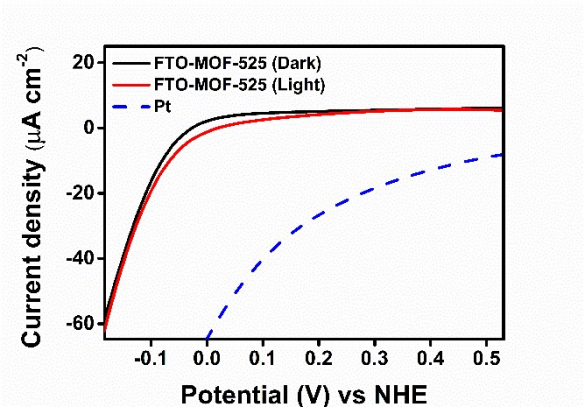

Figure S3. Cathodic Linear sweep voltammetry (LSV) curves on Pt electrode (dotted blue) and FTO-MOF-525 in the dark (black) and in light (red), in 0.1 M $LiClO_4$ acetonitrile solution containing 11 M water, at a scan rate of 50 mV/sec.

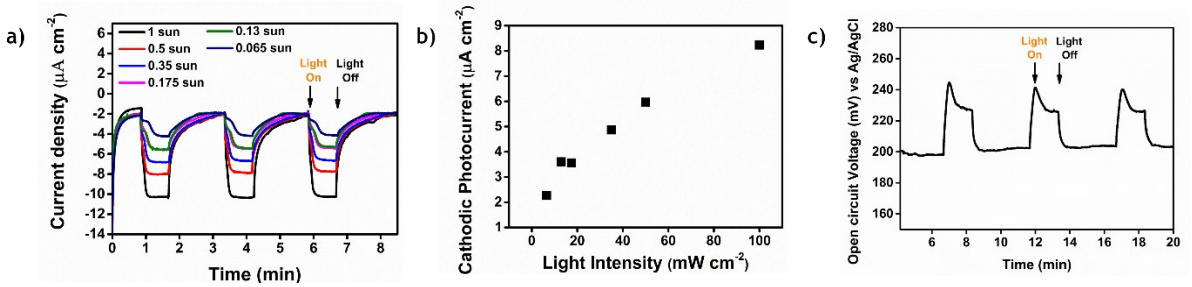

Figure S4. (a) CA at a constant potential of +0.42 V vs NHE at different illumination intensities. (b) photocurrent density as function of light intensity and (c) V_{OC} measurements recorded on the FTO-MOF-525 photo-electrode in 0.1 M $LiClO_4$ acetonitrile solution with 0.1 mM Tetracyanoquinodimethane (TCNQ) while alternatively switching 1 sun of solar illumination on and off (note the arrows).

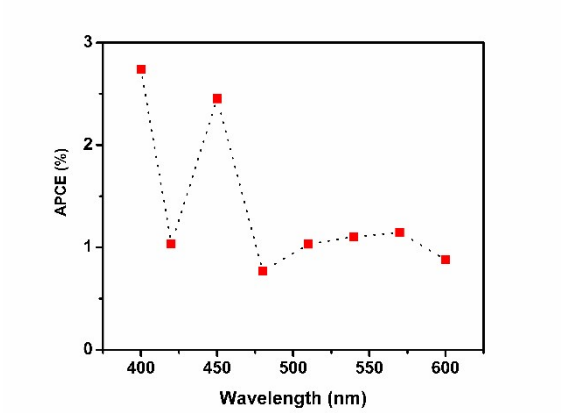

Figure S5. Absorbed photon to current efficiency (APCE) of FTO-MOF-525 photo-anode, measured in 0.1 M $LiClO_4$ acetonitrile solution containing 0.25 M TEOA.

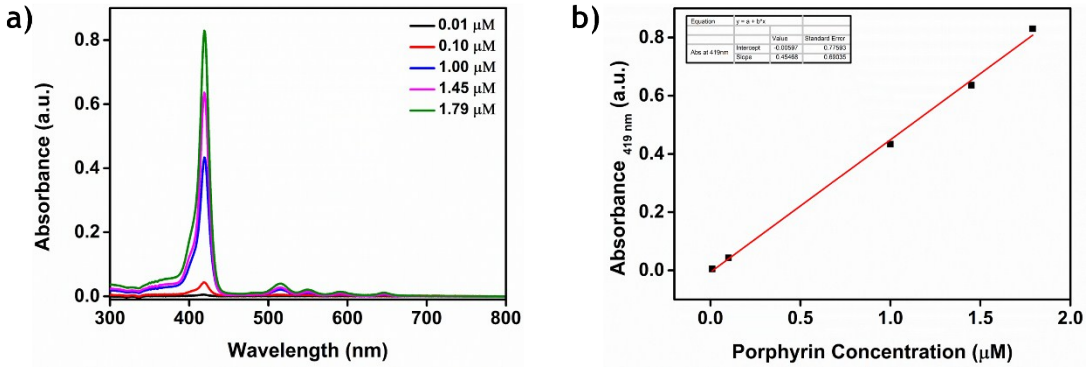

Figure S6. (a) UV-Vis absorbance spectra of TCPP at different concentrations in DMF. (b) Calibration curve of TCPP absorbance at 419 nm as function of its concentration.

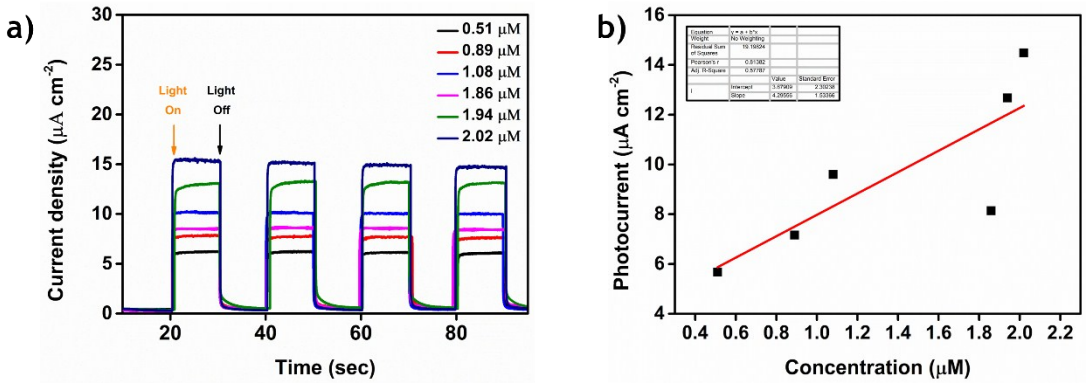

Figure S7. (a) chronoamperometric (CA) measurements of FTO-MOF-525 electrodes containing different surface concentrations of MOF-525. The measurements were done in 0.1 M $LiClO_4$ acetonitrile electrolyte solution containing 0.25 M of TEOA, while applying a constant potential of 0.72 V_{NHE} (b) a plot of the photocurrent as function of the TCPP surface-concentration on the electrode.

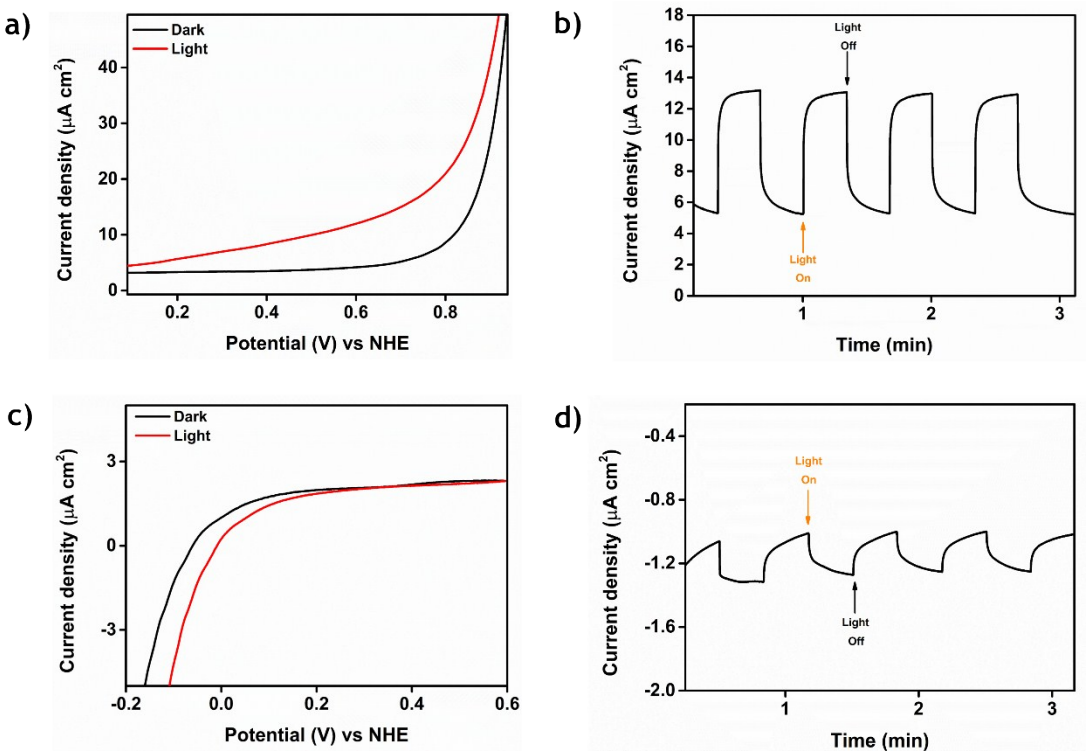

Figure S8. Photo-electrochemical characterization of the FTO-$TCPP_{monolayer}$ electrode (control samples). (a-b) there measurements were performed in 0.1 M $LiClO_4$ acetonitrile solution with 0.25 M TEOA. (a) Linear sweep voltammetry (LSV) measurements were recorded scanning the potential towards the anodic direction at a scan rate of 10 mV/s in the presence (red line) and absence (black line) of 1 sun solar radiation. (b) chronoamperometric (CA) measurement recorded by applying a potential of +0.72 V_{NHE} while alternatively switching the light on and off (note the arrows) (c-d) measurements were performed in 0.1 M $LiClO_4$ acetonitrile solution with 11 M of deionized water c) LSV was recorded scanning the potential in the cathodic direction, at a scan rate of 10 mV/s in the presence (red line) and absence (black line) of 1 sun solar radiation. b) for the CA measurement external potential of 0.02 V_{NHE} was applied while alternatively switching the light on and off (note the arrows).

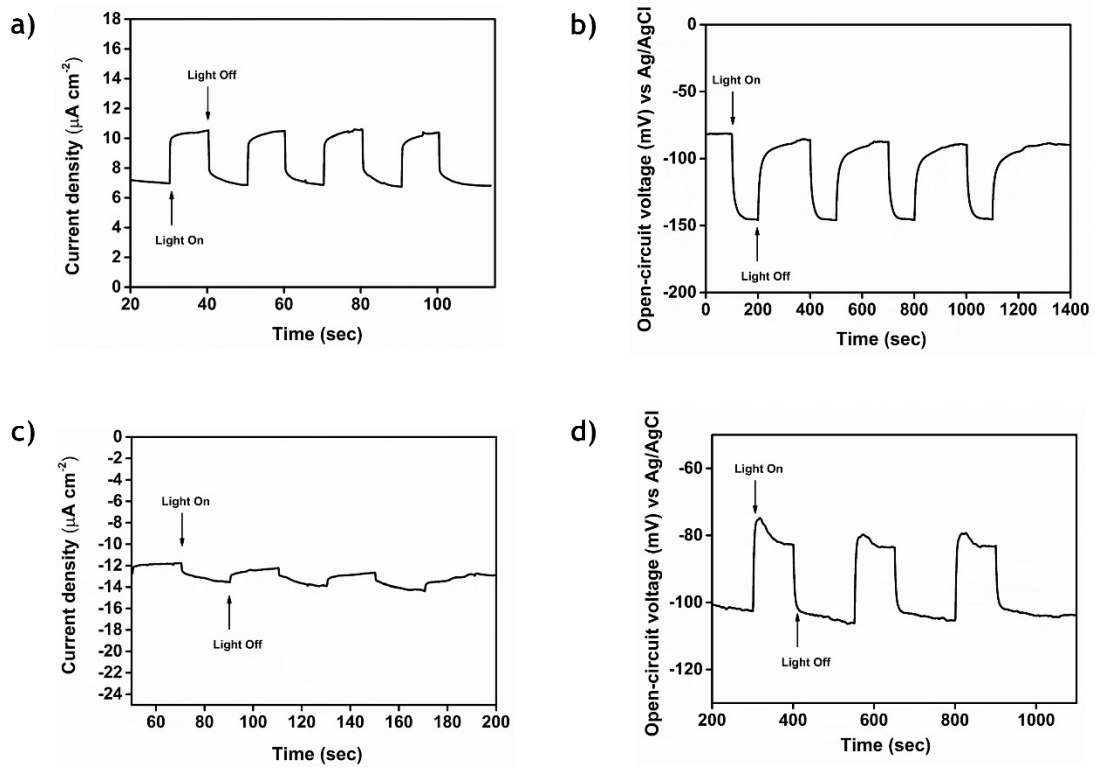

Figure S9. Photo-electrochemical characterization of the FTO-UIO-66@Hemin photo-electrode. Photo-anodic evaluation; (a) CA at 0.5 V vs NHE and (b) VOC in 0.1 M $LiClO_4$ acetonitrile solution with 0.25 M TEOA. Photo-cathodic evaluation; (c) CA at -0.3 V vs NHE and (d) VOC in 0.1 M $LiClO_4$ acetonitrile solution with 11 M water after 20 min oxygen purging (herein, O_2 is acting as the electron accepting species).

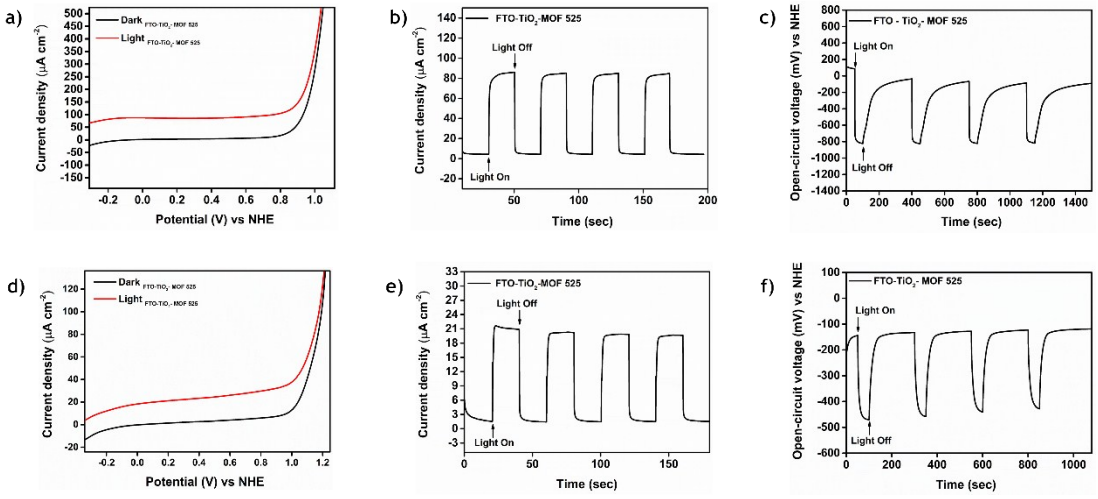

Figure S10. (a) anodic LSV at a scan rate of 50 mV/sec, (b) CA at a constant potential of 0.72 V vs NHE and (c) V_{OC} measurements of the FTO-TiO_2 and FTO-TiO_2-MOF-525 photo-electrodes were recorded in the presence and absence of 1 sun of solar illumination in 0.1 M $LiClO_4$ acetonitrile solution with 0.25 M TEOA. (d) cathodic LSV at a scan rate of 50 mV/sec, (e) CA at a constant potential of 0.02 V vs NHE

and (f) V_{OC} measurements of the FTO-TiO_2 and FTO-TiO_2-MOF-525 photo-electrodes were recorded in the presence and absence of 1 sun of solar illumination in 0.1 M $LiClO_4$ acetonitrile solution with 11 M water.

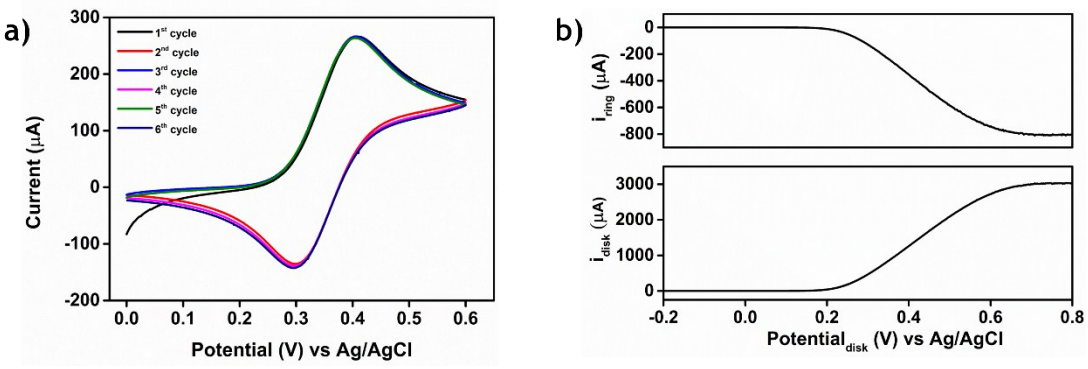

Figure S11. (a) Cyclic voltammetry (CV) scans at 100 mV/s vs Ag/AgCl (KCl sat.) of 1 mM ferrocene in an 0.1 M $LiClO_4$ acetonitrile electrolytic solution (b) Current curves as function of applied potential on the RRDE at 1600 rpm, in order to determine the collection efficiency, N, in a 0.1 M $LiClO_4$ acetonitrile solution containing 1 mM ferrocene. The potential on the disk swept to the anodic direction scanning from -0.2 $V_{Ag/AgCl(KCl\ st.)}$ to +0.8 $V_{Ag/AgCl(KCl\ st.)}$ at a scan rate of 10 mV/s while a constant potential of -0.3 $V_{Ag/AgCl(KCl\ st.)}$ was applied on the ring. In order to determine N the following equation was used; $N = \frac{i_{ring}}{i_{disk}}$, where i_{ring} is the ring current and i_{disk} is disk current. The calculated collection efficiency, N, was determined to be 0.265.

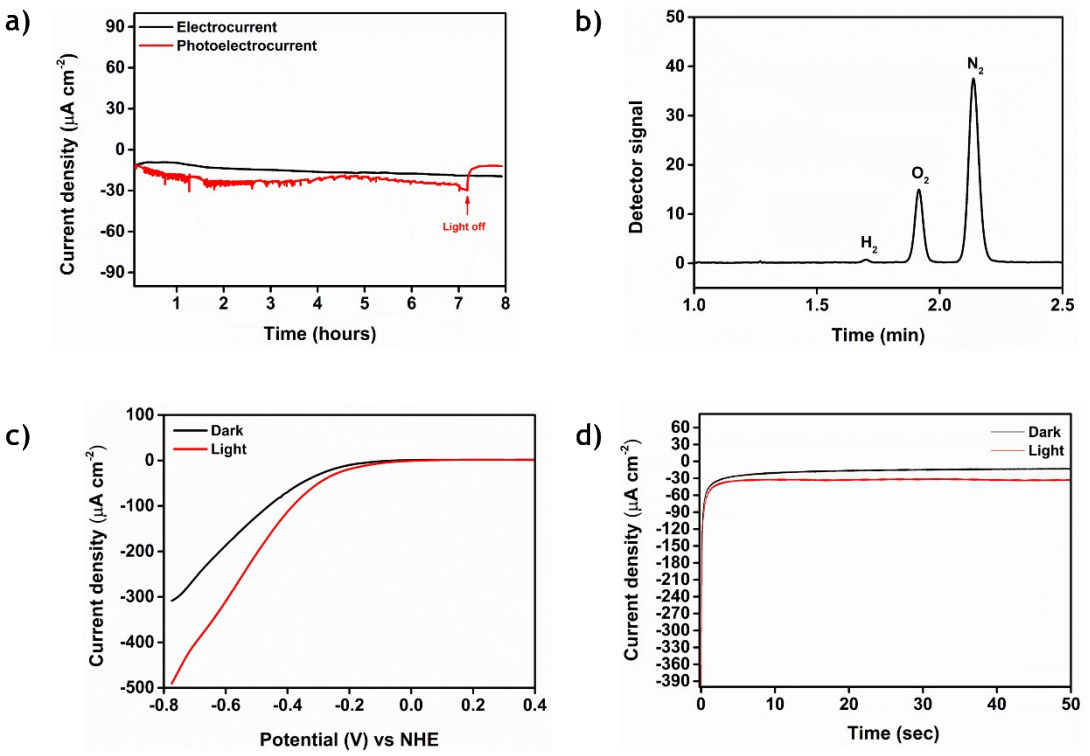

Figure S12. (a) CA curves of the FTO-MOF-525 photo-electrode at a constant potential of -0.8 V_{NHE}. These curves represent a measure of stability of the FTO-MOF-525 photo-cathode. (b) Gas chromatography (GC) analysis of the PEC head space after 7 hours of CA measurements under 1 sun illumination, confirming the formation of molecular hydrogen. (c) Linear sweep voltammetry (LSV) curves of the FTO-MOF-525 photo-electrode. (d) chronoamperometric measurements were recorded on the FTO-MOF-525, while the potential was stepped from 0.2 V to - 0.8 V vs NHE for 60 seconds. All the measurements were conducted in 0.1 M $LiClO_4$ acetonitrile electrolyte solution containing 11 M deionized water and recorded with (red line) and without (black line) 1 sun solar illumination.

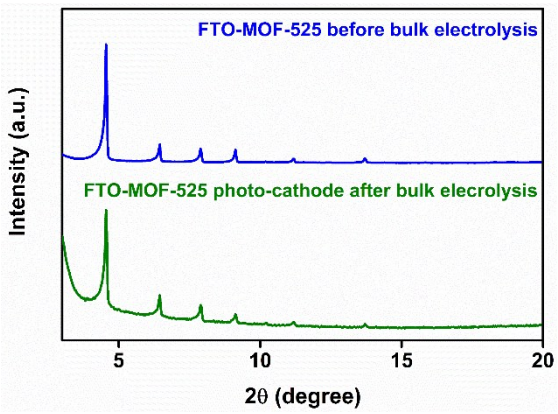

Figure S13. XRD patterns of the FTO-MOF-525 before (blue) and after (green) 7 h of bulk electrolysis.

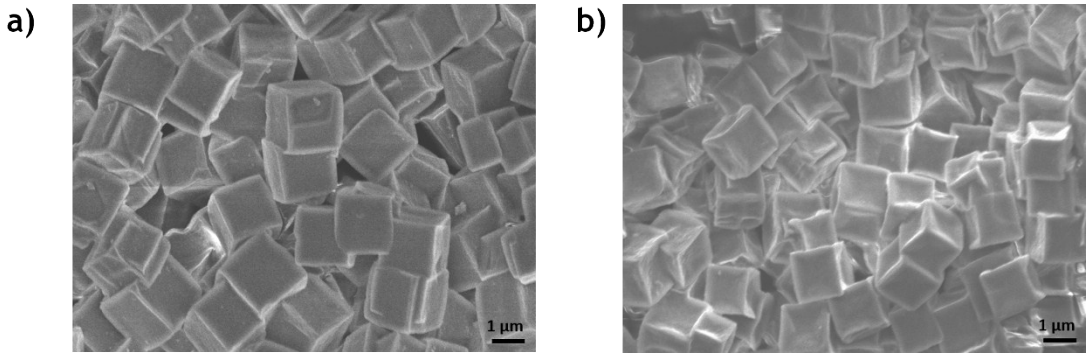

Figure S14. Scanning electron microscopy images of the FTO-MOF-525 electrode before (a) and after (b) 7 h of bulk electrolysis.

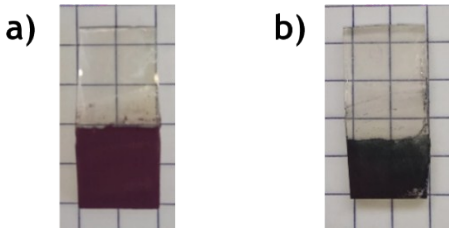

Figure S15. Optical images of the FTO-MOF-525 electrode before (a) and after (b) 7 h of bulk electrolysis.